Full Length Research Paper

Causes of bimodal melting curve:Asymmetric guanine-cytosine (GC) distribution causing two peaks in melting curve and affecting their shapes

Hosein Abtahi[1,2], Mohammad Reza Sadeghi[3], Mohammad Shabani[1], Haleh Edalatkhah[3], Reza Hadavi[3], Mohammad Mehdi Akhondi[4] and Saeed Talebi[3,5]*

[1]Department of Biochemistry, Faculty of Medicine, Tehran University of Medical Sciences, Tehran, Iran.
[2]Department of Basic Sciences, Gonabad University of Medical Sciences, Gonabad, Iran.
[3]Monoclonal Antibody Research Center, Avicenna Research Institute, ACECR, Tehran, Iran.
[4]Reproductive Biotechnology Research Center, Avicenna Research Institute, ACECR, Shahid Beheshti University, Evin, Tehran, Iran.
[5]Department of Medical Genetics, Faculty of Medicine, Tehran University of Medical Sciences, Tehran, Iran.

The aim of this study was to present a new situation in which a relatively single short PCR-product might show two separate peaks with sequence specific shapes at the dissociation curve. SYBR-Green I real-time RT-PCR was performed on Lhcgr-gene transcripts in rats. Different programs were used for melting curve simulation and estimating Tm. Statistical tests were performed to determine whether two peaks at the dissociation curve were belonging to a single template. A bimodal melting curve was observed in real-time RT-PCR on a short segment (169 bp) of Lhcgr gene with a single band in gel electrophoresis. Sequencing of the Cloned PCR-product was compatible with template sequence. Real-time PCR using the vector conveying interested sequence, showed again two peaks at dissociation curve. The GC-content of first 100 bases (75%) and last 69 bases (42%) were significantly different. DNA melting simulation programs also confirmed the bimodal pattern, although, their height and wideness were different to actual peaks. Due to the asymmetric GC distribution effect on dissociation curve in short sequences, it is highly recommended to use DNA melting simulation programs to predict the number of peaks in the melting curve when designating primers; however, predicted peak shapes are not always accurate.

Key words: Asymmetric GC distribution, bimodal melting curve, DNA melting simulation, SYBR-green I real-time PCR.

INTRODUCTION

Real-time PCR is a technique, which measures fluorophore accumulation secondary to DNA amplification. The accumulated fluorophores are different in intercalated dyes, labeled primers, oligonucleotide probes and combination thereof (Holland et al., 1991; Tyagi, 1996; Morrison et al., 1998; Winn-Deen, 1998; Thelwell et al., 2000).

Differentiation of PCR products using DNA melting curve analysis was demonstrated by Ririe et al. (1997) with double-stranded DNA-specific dye SYBR-Green I and II and has since been adopted in real-time PCR applications (Wilhelm and Pingoud, 2003).

DNA melting is co-operative (Beers et al., 1967; Poland, 1974), both sequence and nucleotide position dependent (Blake and Delcourt, 1998); and is also

---

*Corresponding author. E-mail: talebi@avicenna.ac.ir. Tel: +989102116401. Fax: +982122432021.

Abbreviations: **GC**, Guanine-cytosine; **AT**, adenine-thymine; **Lhcgr**, luteinizing hormone/chorionic gonadotropin receptor; **RT**-**PCR**, reverse transcriptase PCR; **bp**, base pair; **Tm**, melting temperature.

subject to smaller local effects (Tostesen et al., 2003; Zeng et al., 2003).

At real-time PCR, using SYBR-Green I as dye, it is expected to have one peak representing one PCR product. Therefore, existing two or more peaks corresponds two or more amplified products.

There are several situations in which two peaks will appear in real-time PCR dissociation curve. These include non-specific amplifications, primer dimers and heterozygote polymorphism.

When there are two different amplified products of nearly the same size with different GC contents, two parted peaks will show two different melting temperatures in which, usually, the lower Tm belongs to the PCR product that has a lower GC content and vice versa.

In some cases, primers added to the PCR mixture might have some interaction with each other. Therefore, we might see primer dimers with a Tm to be very lower than the main Tm of the PCR product.

The idea that large double-stranded DNA fragments of several kilobase-pair may contain several melting domains is not new (Beers et al., 1967). Some authors have stated that bimodal melting curves are sometimes observed for long amplicons (> 200 bp) (Dorak, 2006).

The purpose of this study was to show a situation in which there are two separated peaks at dissociation curve (bimodal melting curve) of a single short PCR-product (<200bp) despite the absence of any non-specific amplification or SNPs. Furthermore, we tried to show the differences between simulation softwares and experimental data concerning the shape of melting peaks.

MATERIALS AND METHODS

To study the Luteinizing hormone receptor gene expression in rat testis, we carried out real-time PCR using our designated primers.

Primer design

According to Swissprot, there are presently, eleven different isoforms recognized for rat Lhcgr gene (http://www.uniprot.org/uniprot/P16235, Retrieved 2010/03/09). Accordingly, we designated a set of primers to recognize all these isoforms.

These primers could be attached to Lhcgr cDNA with accession number of NM_012978.1 at NCBI (http://www.ncbi.nlm.nih.gov/nuccore/6981159, retrieved 2010/03/09). The sense and anti-sense primer sequences were as follow:

Sense: 5'-CAGTCCCGAGAGCTGTCAG-3'
Antisense: 5'-TTACGACCTCATTAAGTCCC-3'

RT-PCR

Adult male Wistar rats (Razi Institute, Iran) were castrated. The harvested testis tissues were ground into fine powder in liquid nitrogen before the extraction of RNA. Total RNA was extracted using RNAzol (Cinna/Biotecx, Friendswood, TX, USA). RNA concentration was measured via UV absorption at 260 nm by a BioPhotometer (Eppendorf, Hamburg, Germany). One microgram of the total RNA was reverse-transcribed to cDNA by using 200 U of Moloney Murine Leukemia Virus (M-MULV) reverse transcriptase enzyme (Fermentase, Vilnius, Lithuania), and 20 pmol of random hexamer primers (Cybergene, Stockholm, Sweden). PCR amplifications of Lhcgr transcripts were performed in the reaction mixture of 25 µl containing 10 to 20 ng of testis cDNA, forward and reverse primers (10 pmol each) specific for Lhcgr transcript, 2.5 µl of PCR buffer (10X), dNTP mixture (0.2 mM each), 1 mM $MgCl_2$, and one unit of taq DNA polymerase (Roche, Mannheim, Germany). Optimization of temperature and $MgCl_2$ were performed to obtain a high quality PCR product. The best result was observed at 60°C with 1 mM of $MgCl_2$.

PCR reactions were carried out using a Mastercycler Gradient thermal cycler (Eppendorf, Hamburg, Germany) indicated as: a preheating cycle at 95°C for 3 min, denaturation at 95°C for 30 s, annealing at 60°C for 30 s, extension at 72°C for 30 s, amplification was performed for 35 cycles, and finally a 7-min cycle at 72°C.

The PCR products were visualized by ethidium bromide staining after electrophoresis in a 1.5% agarose gel, which revealed a single distinct band at 169 bp (Figure 1A). This band was purified using QIA quic Gel Extraction Kit (QIAGEN, Germantown, MD, USA). The purified PCR product was used for sequencing (ABI 3130 genetic analyzer, Applied Biosystems, Foster City, CA, USA) and cloning.

Real-time PCR using SYBR-green I

Real-time quantitative PCR was carried out in 96-well poly-propylene microplates on an ABI Prism 7000 (Applied Biosystems, Foster City, CA, USA) using SYBR-Green I Real-time PCR Master Mix (TAKARA, Otsu, Shiga, Japan) according to the manufacturer's instructions. Amplification was carried out with the following profile: One cycle at 95°C for 10 s, 40 cycles each at 95°C for 5 s and 60°C for 34 s. All PCR reactions were performed in triplicate wells. Specificity of the resulting PCR products was confirmed by melting curves. H_2O was used as the negative control.

### Cloning of Lhcgr in TA vector

The pGEM-T Easy Vector (Promega, Madison, WI, USA) was used for the cloning of the purified PCR product. Ligation reaction was set up using 50 ng of pGEM-T Easy Vector, 3 units of T4 DNA ligase, 75 ng of Lhcgr purified PCR product, and 6 µl of (2X) Rapid Ligation Buffer (Promega). The mixture was incubated at 4°C overnight. Competent cells of E.coli JM109 strain were used for transformation through heat shock method (Howard and Hanga, 2005).

The transformed bacteria were left for one hour in LB broth at 37°C for recovery, and later 100 µl of the transformation culture was cultured onto an ampicillin (100 mg/ml) (Sigma, Louis, MO, USA), IPTG (0.5 mM) (Sigma) and X-gal (80 µg/ml) (Sigma) containing LB agar plate for 16 h at 37°C.

White colonies were screened by 25 cycles of colony PCR using universal primers (SP6 and T7). The recombinant plasmids were isolated from confirmed colonies by using a miniprep kit (QIAGEN, Germantown, MD, USA). Subsequently these extracted vectors were sequenced using ABI Sequencer.

Statistical analysis

To verify whether the GC content along the template was significantly different, we divided all the template sequences into 10- base parts. Statistical analysis was done using SPSS software (V. 13.0). Due to the absence of normal distribution based on Two-Sample Kolmogorov-Smirnov test (P-value = 0.001), Mann-Whitney test was used.
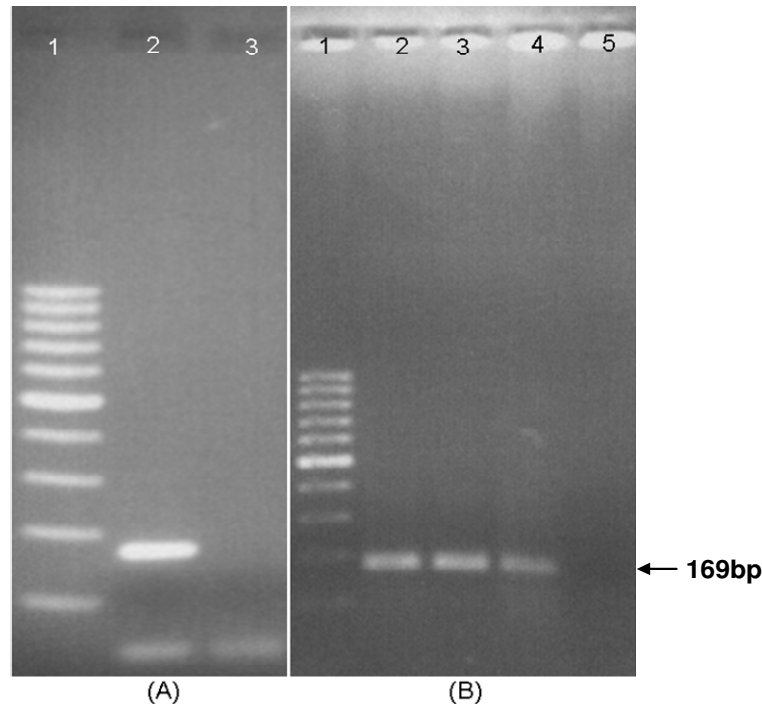
Figure 1. Agarose gel electrophoresis of RT-PCR (A) and real-time PCR (B) products. (A) Lane 1: 100 bp DNA Ladder; lane 2: Lhcgr RT-PCR products; lane 3: H2O as negative control. (B) Lane 1: 100 bp DNA Ladder; lane 2, 3 and 4: Lhcgr real-time PCR products; Lane 5: H2O as negative control. All Lhcgr PCR products showed a band at position 169 bp related to the amplicon size.

Use of DNA melting simulation software

We used two different DNA melting simulation softwares to predict the melting curve of the PCR product: The MeltSim program (http://ftp.bioinformatics.org/pub/meltsim) and the POLAND program (http://www.biophys.uni-duesseldorf.de/local/POLAND/poland.html).

RESULTS

After repeating RT-PCR of Lhcgr transcripts for several times, only one band appeared on agarose gel after electrophoresis of the PCR products (Figure 1A). In real-time PCR for Lhcgr gene expression using testis cDNA, there were two separate peaks in dissociation curve representing two different melting points at 82 and 92.1°C (Figure 2A).

To rule out non-specific amplified products or primer dimers, we tried to optimize the PCR condition. Following decrease in the primer concentration, none of the two peaks did vanish. However, the evaluation of real-time PCR products by gel electrophoresis displayed only one band consequently (Figure 1B). To determine the specificity of primers, the PCR product was cloned in a pGEM-T Easy Vector (Promega, Madison, WI, USA). Sequencing of extracted RT-PCR products and all the minipreped plasmids from three different bacterial

colonies were compatible to Lhcgr gene. To verify if the two peaks in dissociation curve were related to a single sequence, another real-time PCR was run on purified minipreped plasmids. Once again two separate peaks in dissociation curve were observed (Figure 2B).

The GC content differences along 10 base parts sequence of the template showed a sharp drop in the GC content after the subgroup related to 91 to 100 bases from 70 to 40% (Table 1). The GC content was significantly different between the GC-rich (1 to 00 bp) and AT-rich regions (101-169 bp) (P-value = 0.0001). Figures 3A and B depict this difference.

DNA melting simulation softwares MeltSim and POLAND also predicted two separate melting peaks for the aforementioned sequence. In MeltSim, both peaks had the same height and width (Figure 4A). The POLAND software predicted two different curves by two different UV absorbances (260 and 280 nm). The curve for 280 nm was more similar to the observed results in real-time PCR (Figures 2A and 4B).

DISCUSSION

Nearly all different thermal cyclers applied for real-time PCR use a common principle of melting curve preparation. Thermal cyclers increase temperature gradually
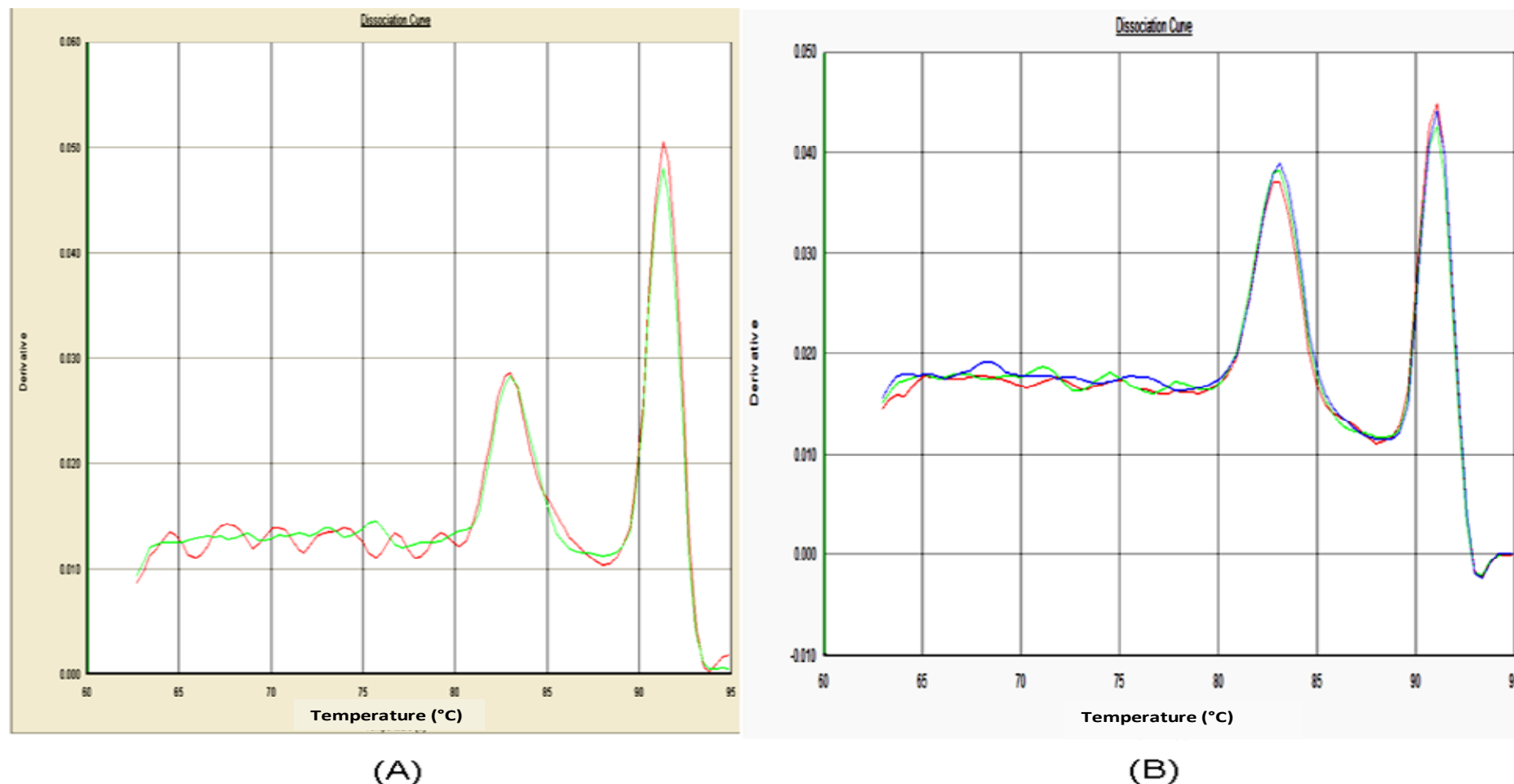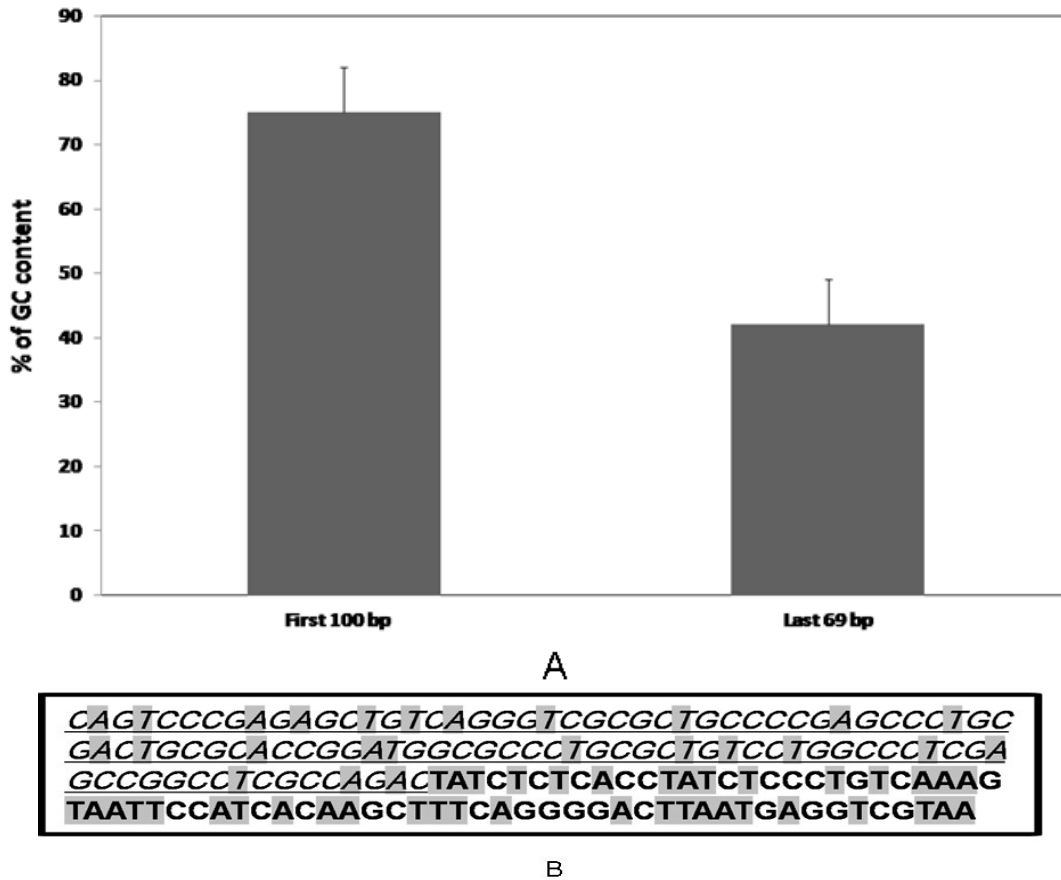
Figure 2. Melting curve analysis of SYBR-Green I real-time PCR on Lhcgr cDNA in duplicate (A) and extracted cloned vectors using Lhcgr primers (B). In both real-time PCR experiments, two separate peaks clearly presented.

up to 99°C and draw a curve with temperature at horizontal axis versus detected signal on the vertical axis. As the temperature increases, the signal decreases due to the dissociation of some double stranded DNA.

Depending on the GC content, melting temperature (Tm), a point in which 50% of dsDNAs are dissociated, is diffe-rent. Clearly, the higher the GC content, the more the dissociation point.

Plotting the minus derivative of fluorescence with respect to temperature (-dF/dT) versus temperature gives us a plot with positive peaks. Each peak is related to each dsDNA in the PCR product. Some of the most important states in

A

CAGTCCCGAGAGCTGTCAGGGTCGCGCTGCCCCGAGCCCTGC
GACTGCGCACCGGATGGCGCCCTGCGCTGTCCTGGCCCCTCGA
GCCGGCCTCGCCAGACTATCTCTCACCTATCTCCCTGTCAAAG
TAATTCCATCACAAGCTTTCAGGGGACTTAATGAGGTCGTAA

B

Figure 3. GC distribution along the template sequence. (A) The comparison of GC content between the two areas (the first 100 bases and the last 69 bases) of template sequence. The GC content was significantly different (P-value = 0.0001) and in (B), showing the entire template, GC-rich sequence is underlined and italic and AT-rich sequence is bolded. Adenine and Thymine bases are highlighted by grey color.
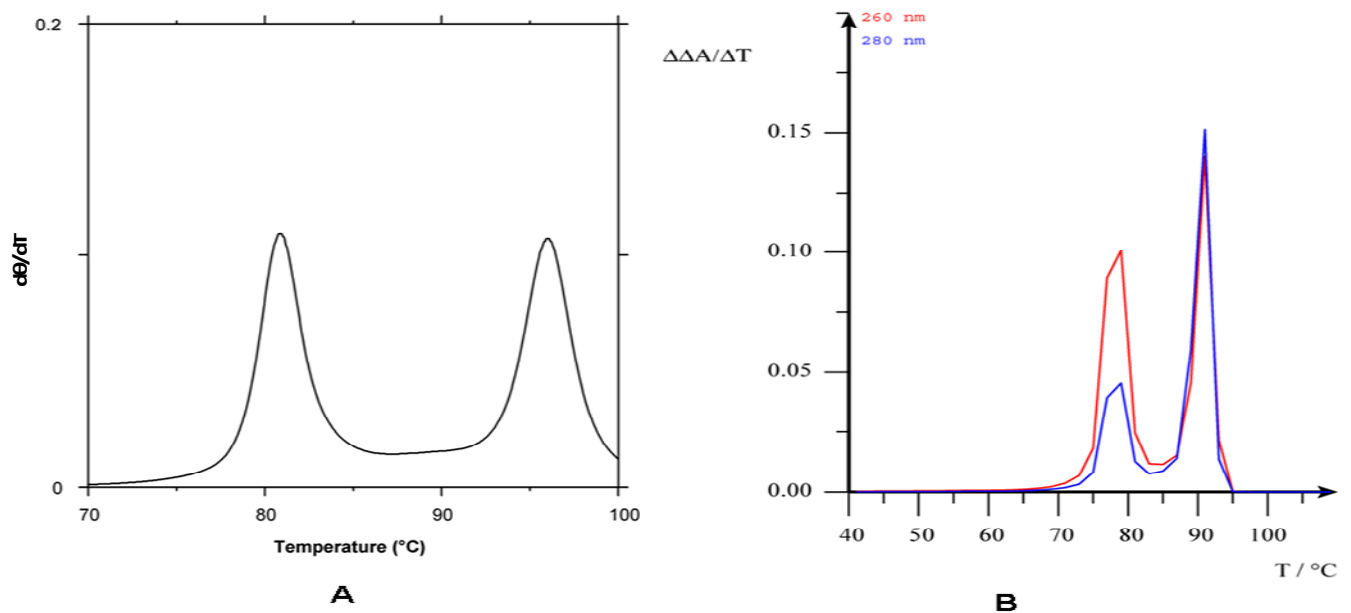
Figure 4. The comparison PCR product melting curves between MeltSim (A), and POLAND (B) softwares.

Table 1. GC content of 10-bp sub-regions of amplicon.

Group	Subgroup	GC%	Mean±SD of GC%	P-value at Mann-Whitney test
1 (First 100 bp)	Bases 1-10	70	75±7.07	
	Bases 11-20	60		
	Bases 21-30	80		
	Bases 31-40	80		
	Bases 41-50	80		
	Bases 51-60	70		
	Bases 61-70	80		
	Bases 71-80	80		
	Bases 81-90	80		0.0001
	Bases 91-100	70		
2 (Last 69 bp)	Bases 101-110	40	42.06±6.98	
	Bases 111-120	50		
	Bases 121-130	30		
	Bases 131-140	40		
	Bases 141-150	50		
	Bases 151-160	40		
	Bases 161-169	44.4		

The amplicon was divided into 10-bp fragments and their GC contents were calculated. Subsequently, according to the GC contents of each sub-region, the amplicon was divided into two areas with significantly different GC content.

which two or more peaks are observed at dissociation curve are non- specific amplifications, primer dimers, real-time multiplex PCR (Guion and Ochoa, 2008), different DNA methylation patterns (Jesper and Guldberg, 2001; Lorente et al., 2008), gene mutation (Aoshima et al., 2000; Nakamura et al., 2009; Rowida et al., 2009), or heterozygote single nucleotide polymor-phisms (Frances et al., 2005).

In this study, melting curve analysis showed two separate peaks at real-time PCR dissociation curve that was completely reproducible. The most possible cause presenting two separate peaks at dissociation curve is non-specific amplification. Although, a combination of gel electrophoresis (Figure 1A) and melting curve analysis (Figure 2A) can always detect the PCR specificity (Dorak, 2006), to further check whether these two peaks belonged to different and relatively similar sequences, the amplicon was cloned into a vector. Following the sequencing of the cloned amplicon, we obtained the exact sequence compatible with Lhcgr gene. Real-time PCR and melting curve analysis on the extracted plasmids verified the purity of the PCR products (Figures 1B and 2B).

The only justification for the observed bimodal peaks is the existence of different GC contents in a single PCR product. Comparing the first 100 and last 69 base pairs, two completely different parts were exhibited in GC content (P-value = 0.0001).

In the melting process of a single PCR product, when the temperature reaches the Tm of the AT-rich area, the two strands of DNA will dissociate and produce a peak at dissociation curve, while the GC-rich area will remain still as double-stranded DNA. As the temperature rises and reaches the Tm of the latter, the rest of the two-stranded DNA dissociates and another peak would appear at the dissociation curve. Considering Blake and Delcourt (1998) findings that the thermodynamic data used in the simulations for base pair stabilities or base stacking are based on empirical data determined for specific salt concentrations in the absence of any intercalating dyes, the difference between the experimental and predicted Tm can be expected. Based on the nature of the inter-action between intercalating dyes and dsDNA (Bjorndal and Fygenson, 2002), it would be expected that intercalating dyes are likely to increase the Tm (Rasmussen et al., 2007).

DNA melting is a very cooperative process (Beers et al., 1967; Poland, 1974), both sequence and nucleotide position dependent (Blake and Delcourt, 1998), and also subject to smaller local effects (Tostesen et al., 2003; Zeng et al., 2003). Primarily, simulation programs, for instance MeltSim, use the aforementioned premises to predict the melting profile of a ds-DNA.

Based on MeltSim, denaturation occurs in several steps, the stability of domains relates to their sequence and their position on dsDNA as well (Blake et al., 1999). These results from the two DNA melting simulation softwares (MeltSim and POLAND) showed that in addition to the mentioned differences, there are differences in the shapes of the peaks (Figure 4). In melting curve obtained from real-time PCR (Figure 2), the peak of the AT rich region is wider than the peak for the

GC-rich area, while both of the used softwares predict the same wide peaks (Figure 4). It is noteworthy to say that the melting curve predicted by POLAND software was more in line with the finding of this study. These observations confirm the idea that the POLAND program is clearly better to model melting curves in similar experiments (Rasmussen et al., 2007).

The second peak from the *in vitro* experiment is taller than the peaks obtained by DNA melting simulation softwares (Figures 2A and 4). This differences could be due to different interaction of dyes with DNA, the GC-preference of SYBR-Green I (Giglio et al., 2003; Wittwer et al., 2003), and the redistribution of SYBR-Green I dye when the first part of the PCR product denatures (Wittwer et al., 2003). Even in some cases, GC-preference to SYBR-Green I, may explain the decrease height or even loss of the peak related to the AT rich region (Rasmussen et al., 2007), although, the presence of GC preference for SYBR-Green I is still controversial (Giglio et al., 2003; Wittwer et al., 2003; Zipper et al., 2004; Gudnason et al., 2007; Colborn et al., 2008).

There is no simple model to accurately describe the melting behavior of ds-DNA as a function of nucleotide content (Alexandrov et al., 2009). The stability of DNA is determined by the interplay of a host of interactions, including hydrogen bonds, aromatic base stacking, backbone conformational constraints and electrostatic interactions, and the coordination of water molecules with metal ions. These interactions strongly depend on DNA structure in a nonlinear fashion.

Finally, it is suggested to consider asymmetric GC distribution as a cause of bimodal melting curve also in short DNA sequences. This is because most primer designing softwares do not consider the GC distribution of amplification sequence; it is highly recommended to use DNA melting simulation programs when designating primers for probe independent real-time PCR.

ACKNOWLEDGMENTS

REFERENCES

Alexandrov BS, Gelev V, Monisova Y, Alexandrov LB , Bishop AR, Rasmussen K, Ush (2009). A nonlinear dynamic model of DNA with a sequence-dependent stacking term. Nucleic Acids Res. 37(7): 2405-2410.

Miyazaki T, Kajita M, Mimura S, Watanabe K, Shimokata K (2000). Rapid detection of deletion mutations in inherited metabolic diseases by melting curve analysis with LightCycler. Clin. Chem. 46(1): 119-122.

Beers W, Cerami A, Reich E (1967). An experimental model for internal denaturation of linear DNA molecules. Proc. Natl. Acad. Sci. USA. 58(4): 1624-1631.

Bjorndal MT, Fygenson DK (2002). DNA melting in the presence of fluorescent intercalating oxazole yellow dyes measured with a gel-based assay. Biopolymers 65(1): 40-44.

Bizzaro JW, Blake JD, Day GR, Delcourt SG, Knowles J, Marx KA, SantaLucia J Jr (1999). Statistical mechanical simulation of polymeric DNA melting with MELTSIM. Bioinformatics, 15(5): 370-375.

Blake RD, Delcourt SG (1998). Thermal stability of DNA. Nucleic Acids Res. 26(14): 3323-3332.

Colborn JM, Byrd BD, Koita OA, Krogstad DJ (2008). Estimation of copy number using SYBR Green: confounding by AT-rich DNA and by variation in amplicon length. Am. J. Trop. Med. Hyg. 79(6): 887-892.

Dorak MT (2006). Real-time PCR. M. T. Dorak. School of Clinical Medical Sciences (Child Health) Newcastle University , Newcastle-upon-Tyne, UK Taylor & Francis Group, p. 104.

Frances F, Corella D, Sorlí JV, Guillén M, González JI, Portolés O (2005). Validating a rapid method for detecting common polymorphisms in the APOA5 gene by melting curve analysis using LightTyper. Clin. Chem. 51(7): 1279-1282.

Giglio S, Monis PT, Saint CP (2003). Demonstration of preferential binding of SYBR Green I to specific DNA fragments in real-time multiplex PCR. Nucleic Acids Res. 31(22): 136.

Gudnaso H, Dufva M, Bang DD, Wolff A, (2007). Comparison of multiple DNA dyes for real-time PCR: effects of dye concentration and sequence composition on DNA amplification and melting temperature. Nucleic Acids Res. 35(19): p. 127.

Guion CE, Ochoa TG, Walker CM, Barletta F, Cleary TG(2008). Detection of diarrheagenic Escherichia coli by use of melting-curve analysis and real-time multiplex PCR. J. Clin. Microbiol. 46(5): 1752-1757.

Holland PM, Abramson RD, Watson R, Gelfand DH (1991). Detection of specific polymerase chain reaction product by utilizing the 5'----3'exonuclease activity of Thermus aquaticus DNA polymerase, Natl. Acad. Sci., 88: p. 7276.

Howard C, Hanga CRB (2005). The chemistry and biology of mucin-type O-linked glycosylation. Bioorganic Medicinal Chem., 13(17): 5021-5034.

Jesper Worm AA, Guldberg P (2001). In-Tube DNA Methylation Profiling by Fluorescence Melting Curve Analysis. Clin. Chem., 47(7): 1183-1189.

Lorente Mueller W, Urdangarín E, Lázcoz P, von Deimling A, Castresana JS (2008). Detection of methylation in promoter sequences by melting curve analysis-based semiquantitative real time PCR. BMC Cancer, 8: p. 61.

Morrison TB, Weis JJ, Wittwer CT(1998). Quantification of low-copy transcripts by continuous SYBR Green I monitoring during amplification. Biotechniques, 24(6): 954-958, 960, 962.

Nakamura S, Yanagihara K, Morinaga Y, Izumikawa K, Seki M, Kakeya H, Yamamoto Y, Kamihira S, Kohno S (2009). Melting curve analysis for rapid detection of topoisomerase gene mutations in Haemophilus influenzae. J. Clin. Microbiol. 47(3): 781-784.

Poland D (1974). Recursion relation generation of probability profiles for specific-sequence macromolecules with long-range correlations. Biopolymers, 13(9): 1859-1871.

Rasmussen JP, Saint CP, Monis PT (2007). Use of DNA melting simulation software for in silico diagnostic assay design: targeting regions with complex melting curves and confirmation by real-time PCR using intercalating dyes. BMC Bioinformatics, 8: 107.

Ririe KM, Rasmussen RP, Wittwer CT (1997). Product differentiation by analysis of DNA melting curves during the polymerase chain reaction. Anal. Biochem. 245(2): 154-160.

Rowida Almomani NVDS, Egbert B, Johan T, den D, Martijn HB, Ieke BG (2009). Rapid and cost effective detection of small mutations in the DMD gene by high resolution melting curve analysis. Neuromuscular Disorders, 19(6): 383-390.

Thelwell N, Millington S, Solinas A, Booth J, Brown T (2000). Mode of action and application of Scorpion primers to mutation detection. Nucleic Acids Res. 28(19): 3752-3761.

Tostesen E, Liu F, Jenssen TK, Hovig E (2003). Speed-up of DNA melting algorithm with complete nearest neighbor properties. Biopolymers, 70(3): 364-376.

Tyagi S, Kramer FR (1996). Molecular beacons: probes that fluoresce upon hybridization. Nat. Biotechnol. 14(3): 303-308.

Wilhelm J, Pingoud A (2003). Real-time polymerase chain reaction,

Weinheim, Germany: Wiley-VCH, c2000-. 4: 1120-1128.

Winn-Deen ES (1998). Direct fluorescence detection of allele-specific PCR products using novel energy-transfer labeled primers. Mol. Diagnosis, 3(4): 217-222.

Wittwer CT, Reed GH, Gundry CN, Vandersteen JG, Pryor RJ (2003). High-resolution genotyping by amplicon melting analysis using LCGreen. Clin. Chem. 49(6 Pt 1): 853-860.

Zeng Y, Montrichok A, Zocchi G (2003). Length and statistical weight of bubbles in DNA melting. Phys. Rev. Lett. 91(14): p. 148101.

Zipper H, Brunner H, Bernhagen J, Vitzthum F (2004). Investigations on DNA intercalation and surface binding by SYBR Green I, its structure determination and methodological implications. Nucleic Acids Res. 32(12): p. 103.